THE JOURNAL OF BIOLOGICAL CHEMISTRY VOL. 281, NO. 5, pp. 2820–2827, February 3, 2006
© 2006 by The American Society for Biochemistry and Molecular Biology, Inc. Printed in the U.S.A.

Proteomic Analysis of β_1-Adrenergic Receptor Interactions with PDZ Scaffold Proteins*[S]

Received for publication, August 29, 2005, and in revised form, November 8, 2005 Published, JBC Papers in Press, November 29, 2005, DOI 10.1074/jbc.M509503200

Junqi He[‡1], Michele Bellini[§1], Hiroyuki Inuzuka[§], Jianguo Xu[§], Ying Xiong[‡], Xiaomei Yang[‡], Amanda M. Castleberry[§], and Randy A. Hall[§2]

From the [‡]Department of Biochemistry and Molecular Biology, Capital University of Medical Sciences, Beijing 100054, China and the [§]Department of Pharmacology, Rollins Research Center, Emory University, School of Medicine, Atlanta, Georgia 30322

Many G protein-coupled receptors possess carboxyl-terminal motifs ideal for interaction with PDZ scaffold proteins, which can control receptor trafficking and signaling in a cell-specific manner. To gain a panoramic view of β_1-adrenergic receptor (β_1AR) interactions with PDZ scaffolds, the β_1AR carboxyl terminus was screened against a newly developed proteomic array of PDZ domains. These screens confirmed β_1AR associations with several previously identified PDZ partners, such as PSD-95, MAGI-2, GIPC, and CAL. Moreover, two novel β_1AR-interacting proteins, SAP97 and MAGI-3, were also identified. The β_1AR carboxyl terminus was found to bind specifically to the first PDZ domain of MAGI-3, with the last four amino acids (E-S-K-V) of β_1AR being the key determinants of the interaction. Full-length β_1AR robustly associated with full-length MAGI-3 in cells, and this association was abolished by mutation of the β_1AR terminal valine residue to alanine (V477A), as determined by co-immunoprecipitation experiments and immunofluorescence co-localization studies. MAGI-3 co-expression with β_1AR profoundly impaired β_1AR-mediated ERK1/2 activation but had no apparent effect on β_1AR-mediated cyclic AMP generation or agonist-promoted β_1AR internalization. These findings revealed that the interaction of MAGI-3 with β_1AR can selectively regulate specific aspects of receptor signaling. Moreover, the screens of the PDZ domain proteomic array provide a comprehensive view of β_1AR interactions with PDZ scaffolds, thereby shedding light on the molecular mechanisms by which β_1AR signaling and trafficking can be regulated in a cell-specific manner.

Cellular responses to a given hormone or neurotransmitter can vary markedly between different types of cells. In many cases, such cellular differences are because of differential expression of receptor subtypes. However, even cells expressing exactly the same receptor subtypes can exhibit distinct responses to a given ligand, because receptors often behave quite differently in distinct cellular environments. The trafficking and signaling properties of G protein-coupled receptors (GPCRs),[3] which comprise the largest family of cell surface receptors, are known to be especially influenced by cellular context. The activity of a GPCR depends not only on the complement of downstream effectors expressed in a given cell but also on the set of expressed G proteins, kinases, and scaffold proteins that directly interact with the receptor to shape its signaling capability.

PDZ scaffolds comprise a key class of GPCR-interacting proteins that can strongly influence receptor trafficking and signaling. The term PDZ is derived from the names of the first three proteins in which these domains were first identified: the post-synaptic density protein PSD-95, the *Drosophila* protein Discs-large, and the tight junction protein ZO-1. PDZ domains are ~90 amino acids in length and bind to specific carboxyl-terminal motifs on their target proteins. There are three general classes of PDZ domain: Class I domains, which recognize the carboxyl-terminal motif S/T-*X*-ϕ (where "ϕ" indicates a hydrophobic amino acid and "*X*" indicates any amino acid), Class II domains, which recognize the carboxyl-terminal motif ϕ-*X*-ϕ, and Class III domains, which recognize D/E-*X*-ϕ as their preferred carboxyl-terminal motif (1).

Many GPCRs possess carboxyl-terminal motifs appropriate for interaction with PDZ domains. One subfamily of GPCRs for which there are already several reports of PDZ interactions is the subfamily of β-adrenergic receptors (βARs). This subfamily includes the closely related subtypes β_1AR, β_2AR, and β_3AR and mediates physiological responses to epinephrine and norepinephrine (2). It has been shown that several Class I PDZ proteins associate with the carboxyl terminus (CT) of β_1AR, including PSD-95 (postsynaptic density-95) (3–5), MAGI-2 (membrane-associated guanylate kinase inverted-2) (4), CNrasGEF (cAMP-dependent guanine nucleotide exchange factor, also known as PDZ-GEF1) (6), GIPC (GAIP-interacting protein, carboxyl terminus) (7), and CAL (cystic fibrosis transmembrane conductance regulator-associated ligand, also known as GOPC or FIG) (8). MAGI-2 and PSD-95 are structurally related PDZ proteins of the membrane-associated guanylate kinase-like (MAGUK) family, but nonetheless they exhibit diametrically opposing effects on agonist-induced β_1AR internalization; MAGI-2 strongly promotes β_1AR internalization (4), whereas PSD-95 markedly inhibits it (3, 4). In contrast, CNrasGEF and GIPC have no obvious effects on β_1AR endocytosis but rather regulate various aspects of β_1AR signaling (6, 7), whereas the Golgi-associated protein CAL directs β_1AR anterograde trafficking through the endoplasmic reticulum-Golgi complex to the plasma membrane (8). Interestingly, despite the high degree of overall sequence similarity between β_1AR and β_2AR, none of the aforementioned β_1AR-associated PDZ proteins interact with β_2AR.

* This work was supported by grants from the National Institutes of Health and a Distinguished Young Scholar in Medical Research award from the W. M. Keck Foundation (to R. A. H.) and by Grants 30572183 and 30371643 from the National Natural Science Foundation of the People's Republic of China (to J. H.). The costs of publication of this article were defrayed in part by the payment of page charges. This article must therefore be hereby marked "*advertisement*" in accordance with 18 U.S.C. Section 1734 solely to indicate this fact.

[S] The on-line version of this article (available at http://www.jbc.org) contains supplemental information.

[1] Both authors contributed equally to this work.

[2] To whom correspondence should be addressed: Dept. of Pharmacology, Emory University School of Medicine, 5113 Rollins Research Center, 1510 Clifton Rd. Atlanta, GA 30322. Tel.: 404-727-3699; Fax: 404-727-0365; E-mail: rhall@pharm.emory.edu.

[3] The abbreviations used are: GPCR, G protein-coupled receptor; PDZ, PSD-95/Discs-large/ZO-1 homology; PSD-95, postsynaptic density protein of 95 kDa; βAR, β-adrenergic receptor; MAGI, membrane-associated guanylate kinase-like protein with an inverted domain structure; CNrasGEF, cAMP-dependent guanine nucleotide exchange factor; GIPC, GAIP-interacting protein, carboxyl terminus; CAL, cystic fibrosis transmembrane conductance regulator-associated ligand; NHERF, Na^+/H^+ exchanger regulatory factor; GST, glutathione *S*-transferase; CT, carboxyl terminus; HA, hemagglutinin; HEK, human embryonic kidney; PBS, phosphate-buffered saline; ERK, extracellular signal-related kinase.

Instead, β_2AR has been shown to interact with the Na^+/H^+-exchanger regulatory factors NHERF-1 (also known as EBP50) and NHERF-2 (also known as E3KARP) (9–11). These interactions mediate regulation of Na^+/H^+ exchange by β_2AR (9) and also dictate β_2AR postendocytic sorting following agonist-promoted internalization (11).

It has been known for many years that β_1AR exhibits differential behavior in distinct cellular environments, with tissue-specific differences in the rate of receptor endocytosis being particularly pronounced (12–15). Such differences in β_1AR behavior in distinct cells may be explained in large part by the differential expression of β_1AR-interacting proteins such as PDZ scaffolds, which as described above can strongly regulate β_1AR trafficking and activity. Thus, it is a point of clear physiological interest to determine the full set of PDZ scaffolds that can associate with β_1AR. There are ~440 PDZ domains in the human proteome, with ~25% of these being probable Class I PDZ domains (1). We have recently prepared the majority of known or probable Class I PDZ domains as hexahistidine-tagged fusion proteins and arranged them on a proteomic array to facilitate the rapid analysis of PDZ domain-mediated interactions (16). Here, we screened this PDZ domain array with the β_1AR-CT resulting in the confirmation of several known β_1AR/PDZ interactions as well as the elucidation of several novel interactions. Furthermore, one of the novel interactions, the association between β_1AR and MAGI-3, was found to occur in a cellular context and to also regulate β_1AR signaling activity.

EXPERIMENTAL PROCEDURES

Preparation of Plasmids and Fusion Proteins—The β_1AR and β_2AR carboxyl termini (the last 30 amino acids of the human β_1- and β_2-adrenergic receptors) were amplified via PCR and subcloned into pGEX-4T-1 for expression as GST fusion proteins. Point mutations of both β_1AR-CT and full-length Flag-β_1AR construct (V477A) were introduced via PCR and verified by ABI sequencing. The full-length V5/His-MAGI-3 construct in pcDNA3 was kindly provided by Rich Laura (Genentech). The individual PDZ domains of MAGI-3, and all of the other PDZ domains utilized on the PDZ array, were amplified via PCR and inserted into pET30A for expression as His/S-tagged fusion proteins, as described (16).

PDZ Array Overlay Assay—Gridded nylon membranes were spotted with His/S-tagged PDZ domain fusion proteins (1 μg/bin), as described (16). The membranes were placed at room temperature for 24 h to dry and then stored at 4 °C for later use. Prior to experiments, membranes were blocked in blot buffer for 30 min at room temperature then overlaid with 100 nM GST fusion proteins in blot buffer for 1 h at room temperature. The arrays were washed three times with blot buffer, and incubated with an horseradish peroxidase-conjugated anti-GST antibody (1:3000, Amersham Biosciences). Interactions of the GST fusion proteins with the various PDZ domains were then visualized via chemiluminescence using the ECL kit (Pierce).

Blot Overlay Assay—The binding of receptor carboxyl terminus-GST fusion proteins to His/S-tagged PDZ domain fusion proteins was assayed via a blot overlay technique. The receptor CT-GST fusion proteins (1 μg/lane) were run on 4–20% SDS-polyacrylamide gels (Novex, San Diego, CA), blotted, and overlaid with the His/S-tagged PDZ domains (50 nM final concentration) in blot buffer for 1 h at room temperature. The blots were then washed three times with blot buffer and incubated with S-protein horseradish peroxidase conjugate (Novagen, 1:4000) for 1 h at room temperature and were visualized via chemiluminescence as described above.

GST Fusion Protein Pull-down Assay—GST fusion proteins were purified from bacteria using glutathione-Sepharose 4B beads (Sigma) according to the manufacturer's protocol and resuspended in PBS containing 0.5% Nonidet P-40 and protease inhibitors. Equal amounts of GST fusion proteins (conjugated on beads) were incubated with 1 ml of clarified whole cell extracts from COS-7 cells transfected with His/V5-MAGI-3. After incubation at 4 °C with gentle rotation for 4 h, the beads were extensively washed with ice-cold PBS containing 0.5% Nonidet P-40. Proteins were eluted from the beads with SDS-PAGE sample buffer, resolved on SDS-polyacrylamide gels, and transferred to nitrocellulose. MAGI-3 was then detected via Western blotting with the monoclonal anti-V5 antibody followed by a horseradish peroxidase-conjugated anti-mouse IgG secondary antibody (1:2000).

Cell Culture and Transfection—All tissue culture medium and related reagents were purchased from Invitrogen. HEK-293 and COS-7 cells were maintained in complete medium (Dulbecco's modified eagle medium plus 10% fetal bovine serum and 1% penicillin/streptomycin) in a 37 °C/5% CO_2 incubator. For transfections, 1 μg of total DNA was mixed with Lipofectamine 2000 (15 μl) (Invitrogen) and added to 5 ml of complete medium in 10-cm tissue culture plates containing cells at ~50–80% confluency. Following a 4-h incubation, fetal bovine serum was added to the medium to 10%, and cells were then harvested after 48 h.

Western Blotting and Antibodies—Samples were run on 4–20% SDS-polyacrylamide gels (Invitrogen) for 1 h at 150 V and then transferred to nitrocellulose. The blots were blocked in "blot buffer" (2% nonfat dry milk, 0.1% Tween 20, 50 mM NaCl, 10 mM Hepes, pH 7.4) for at least 30 min and then incubated with primary antibody in blot buffer for 1 h at room temperature. The blots were then washed three times with 10 ml of blot buffer each and incubated for 30 min at room temperature with a horseradish peroxidase-conjugated secondary antibody (Amersham Biosciences) in blot buffer. Finally, the blots were washed three more times with 10 ml of blot buffer each and visualized via enzyme-linked chemiluminescence as described above. Horseradish peroxidase-conjugated anti-GST, polyclonal anti-His, and horseradish peroxidase-conjugated anti-mouse IgG and anti-rabbit IgG secondary antibodies were purchased from Amersham Biosciences. Monoclonal anti-V5 was from Invitrogen, and monoclonal anti-hemagglutinin (HA) 12CA5 antibody was from Roche Molecular Biochemicals. Polyclonal anti-MAGI-3, anti-FLAG M2 monoclonal antibody, and anti-FLAG M2 affinity gel were from Sigma. Polyclonal anti-β_1AR (V-19) was purchased from Santa Cruz.

Immunoprecipitation—Cells were harvested in ice-cold solubilization buffer (10 mM Hepes, 50 mM NaCl, 5 mM EDTA, 1 mM benzamidine, 0.5% Triton X-100) and incubated end-over-end at 4 °C for 1 h to achieve solubilization. Particulate matter was removed via centrifugation for 15 min at 15,000 × *g* (4 °C). The solubilizates were then incubated with 30 μl of anti-FLAG M2 affinity gel (for transfected cells) or 30 μl of protein A/G-agarose plus 5 μl of polyclonal anti-β_1AR antibody (for brain lysates) for 2 h with end-over-end rotation at 4 °C. After five washes with 1.0 ml of ice-cold solubilization buffer, the immunoprecipitated proteins were eluted from the beads via incubation with SDS-PAGE sample buffer and visualized via Western blot using appropriate antibodies.

Cell Surface Expression Assay—Receptor expression in the plasma membrane was quantified as described (17). Briefly, cells were grown in 35-mm dishes and incubated in the absence and presence of agonist. The cells were then rinsed in PBS and fixed with 4% paraformaldehyde in PBS for 30 min and then rinsed three more times in PBS and blocked with blocking buffer (2% nonfat dry milk in PBS) for at least 30 min. The fixed cells were incubated with primary antibody in blocking buffer for 1 h at room temperature. The dishes were subsequently washed three

times with 2 ml of block buffer and incubated for 1 h at room temperature with horseradish peroxidase-conjugated secondary antibody in blocking buffer. Finally, the dishes were washed three times with 2 ml of blocking buffer and one time with 2 ml of PBS and incubated with 2 ml of ECL reagent for exactly 15 s. The luminescence, which corresponds to the amount of receptor on the cell surface, was determined by using a TD 20/20 luminometer.

Immunofluorescence Microscopy—HEK-293 cells were transiently transfected with combinations of Flag-β_1AR, Flag-V477A, and/or V5/His-MAGI-3. Forty-eight hours after transfection, cells were washed three times with Dulbecco's PBS and then fixed in 4% paraformaldehyde in PBS for 30 min at room temperature. To visualize the subcellular localization of β_1AR and MAGI-3, cells were blocked and permeabilized with a buffer containing 2% bovine serum albumin and 0.04% saponin in PBS ("saponin buffer") for 30 min at room temperature. The cells were then incubated with mouse monoclonal anti-FLAG and rabbit polyclonal anti-His antibodies for 1 h at room temperature. After three washes (1 min) with saponin buffer, the cells were incubated with a rhodamine red-conjugated anti-mouse IgG at 1:200 dilution and fluorescein isothiocyanate-conjugated anti-rabbit IgG at 1:200 dilution (Jackson ImmunoResearch Laboratories) for 1 h at room temperature. After three washes (1 min) with saponin buffer and one wash with PBS, coverslips were mounted and rhodamine red-labeled β_1AR and fluorescein isothiocyanate-labeled MAGI-3 were visualized with a Zeiss LSM-410 laser confocal microscope. Multiple control experiments, utilizing either transfected cells in the absence of primary antibody or untransfected cells in the presence of primary antibody, revealed a very low level of background staining, indicating that the primary antibody-dependent immunostaining observed in the transfected cells was specific.

Phospho-ERK Assay—Twenty-four hours after transfection, cells were split into 6-well dishes and incubated in serum-free medium overnight prior to experiments. Agonist stimulation was performed at 37 °C in serum-free media for 5 min. The medium was removed, and cells were then harvested in SDS-PAGE sample buffer. The samples were sonicated briefly and analyzed via SDS-PAGE. The levels of p42/44 ERK phosphorylation were visualized by Western blot using an anti-phospho-ERK1/2 antibody (Cell Signaling Technology), whereas the levels of total ERK in the same lysates were assessed using an anti-ERK antibody (Cell Signaling Technology). Immunoreactive bands were visualized via chemiluminescence and quantified using NIH Image 1.62. For each sample, the level of phospho-ERK immunoreactivity was normalized to total ERK immunoreactivity. Variation in total ERK immunoreactivity between samples was typically very small (<10%), so only a small amount of normalization was required in each experiment.

RESULTS

Proteomic Analysis of β_1AR/PDZ Interactions—To obtain a panoramic view of the set of PDZ domains that bind to β_1AR, a GST fusion protein corresponding to the β_1AR-CT was purified and subsequently used in overlay experiments. Individual His/S-tagged fusion proteins of 96 distinct PDZ domains were purified and spotted on a gridded nylon membrane (1 μg of fusion protein/bin) and then overlaid with purified β_1AR-CT-GST (100 nM). As shown in Fig. 1, β_1AR-CT did not bind to the majority of PDZ domains on the array but rather bound strongly to a handful of specific PDZ domains. These included MAGI-1 PDZ1 (bin A1), MAGI-2 PDZ1 and PDZ2 (A5-A6), PSD-95 PDZ3 (B8), CAL PDZ (B10), and GIPC PDZ (D8), which are PDZ domains that have previously been reported to bind to β_1AR-CT (3, 4, 7, 8). The overlays of the PDZ array also revealed β_1AR-CT interactions with MAGI-3 PDZ1 (A10) and SAP97 PDZ3 (C3), which have not previously been shown to interact with β_1AR. In matching control membranes where GST alone was overlaid onto the array, no binding of GST was detectable (data not shown), demonstrating the low amount of nonspecific binding in these assays. Because the interaction of β_1AR-CT with MAGI-3 PDZ1 was consistently the most robust association observed, we decided to characterize this interaction further and assess its functional significance.

Structural Determinants of the β_1AR-CT Interaction with MAGI-3 PDZ1—The binding of MAGI-3 PDZ1 to various point-mutated versions of the β_1AR-CT was examined in overlay experiments (Fig. 2*A*, *lanes 1–6*). The wild-type amino acid sequence of β_1AR is SESKV. The mutation to Ala of the terminal Val residue, as well as Ser at the −2 position, completely blocked binding to MAGI-3 PDZ1. In addition, the mutation of Glu at the −3 position also impaired the interaction. However, mutation to Ala at the −1 and −4 positions had little effect. To further characterize the structural determinants of this interaction, we mutated the wild-type SESKV to SESRV, SETKV, and STSKV and examined the binding of these mutant fusion proteins to MAGI-3 PDZ1 (Fig. 2*A*, *lanes 7–9*). The mutation to Thr at the −3 position and Arg at −1 strongly inhibited binding, but the mutation to Thr at the −2 position had little effect on the interaction. These findings revealed a selective inhibition of binding to MAGI-3 PDZ1 by specific point mutations to three of the last five amino acids of the β_1AR-CT.

To examine the binding of the β_1AR-CT to full-length MAGI-3 rather than simply the isolated PDZ1 domain, HEK-293 cells were transfected with full-length V5/His-tagged MAGI-3, and pull-down assays were performed using purified GST fusion proteins corresponding to β_1AR-CT with the terminal Val residue mutated to either Ala, Ile, Met, or Leu (Fig. 2*B*). Each of these mutations completely abolished the interaction between MAGI-3 and β_1AR-CT, revealing a critical importance of the terminal Val residue in mediating the β_1AR/MAGI-3 interaction.

β_1AR and MAGI-3 Associate in Cells—We next examined the interaction between full-length β_1AR and full-length MAGI-3 in a cellular context. HEK-293 cells were transfected with V5/His-MAGI-3 and either Flag-β_1AR or Flag-V477A, a mutant receptor with the terminal Val changed to Ala. Co-immunoprecipitation experiments were performed in the presence and absence of stimulation with the βAR-selective agonist isoproterenol (Fig. 3*A*). MAGI-3 co-immunoprecipitated with β_1AR, and the amount of co-immunoprecipitation did not significantly change when β_1AR was stimulated with agonist for 15 min. No co-immunoprecipitation was observed, however, between the V477A mutant receptor and MAGI-3, revealing the importance of the terminal Val residue for the cellular interaction of β_1AR and MAGI-3.

In addition to the transfection experiments, we also studied the interactions of full-length endogenous β_1AR and MAGI-3 in various native tissues, including brain, heart, and kidney. Solubilized lysates derived from these tissues were incubated with an anti-β_1AR antibody linked to protein A/G-agarose beads, and the resultant immunoprecipitates were probed via Western blot for MAGI-3 co-immunoprecipitation using an anti-MAGI-3 antibody. Robust co-immunoprecipitation of MAGI-3 with β_1AR was observed from all three tissues (Fig. 3*B*). These data reveal the existence of a physical complex between β_1AR and MAGI-3 in native tissues where neither protein is overexpressed.

The potential co-localization of β_1AR and MAGI-3 in cultured cells was examined via immunofluorescence microscopy (Fig. 4). HEK-293 cells were transfected with V5/His-MAGI-3 and/or Flag-β_1AR or Flag-V477A. When expressed alone, β_1AR and the V477A mutant receptor were both predominantly localized to the plasma membrane (Fig. 4*A*), whereas MAGI-3 expressed alone was found predominantly in the nucleus, with light cytoplasmic staining also evident (Fig. 4*B*). Strikingly,

A

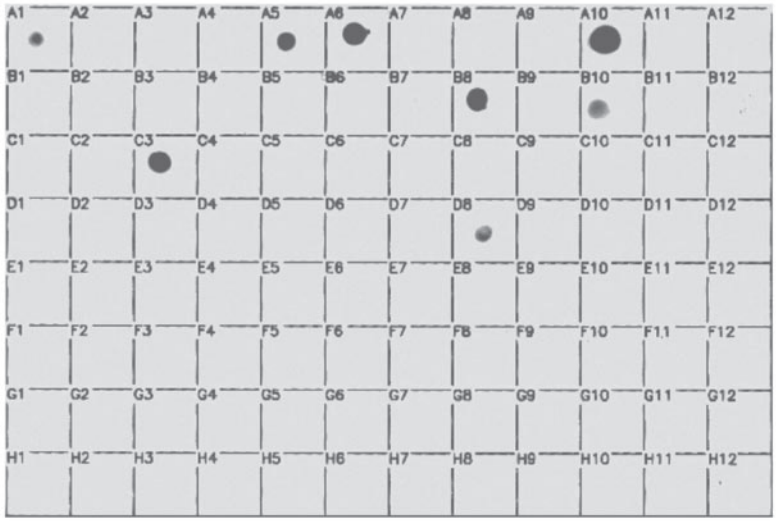

B

Bin	PDZ Domain	Bin	PDZ Domain	Bin	PDZ Domain
A1	MAGI-1 PDZ1	C9	ERBIN PDZ	F5	MUPP1 PDZ10
A2	MAGI-1 PDZ2	C10	ZO-1 PDZ1	F6	MUPP1 PDZ12
A3	MAGI-1 PDZ3	C11	ZO-1 PDZ2	F7	MUPP1 PDZ13
A4	MAGI-1 PDZ4+5	C12	ZO-1 PDZ3	F8	PTPN13 PDZ1
A5	MAGI-2 PDZ1	D1	ZO-2 PDZ1	F9	PTPN13 PDZ3
A6	MAGI-2 PDZ2	D2	ZO-2 PDZ2	F10	PTPN13 PDZ4+5
A7	MAGI-2 PDZ3	D3	ZO-2 PDZ3	F11	PDZK1 PDZ1
A8	MAGI-2 PDZ4	D4	ZO-3 PDZ1	F12	PDZK1 PDZ2
A9	MAGI-2 PDZ5	D5	ZO-3 PDZ2	G1	PDZK1 PDZ3
A10	MAGI-3 PDZ1	D6	ZO-3 PDZ3	G2	PDZK1 PDZ4
A11	MAGI-3 PDZ2	D7	C2PA PDZ	G3	PDZK2 PDZ1
A12	MAGI-3 PDZ3	D8	GIPC PDZ	G4	PDZK2 PDZ2
B1	MAGI-3 PDZ4	D9	MALS-1 PDZ	G5	PDZK2 PDZ3
B2	MAGI-3 PDZ5	D10	MALS-3 PDZ	G6	PDZK2 PDZ4
B3	NHERF-1 PDZ1	D11	Densin-180 PDZ	G7	LNX1 PDZ1
B4	NHERF-1 PDZ2	D12	Rhophilin-1 PDZ	G8	LNX1 PDZ2
B5	NHERF-2 PDZ1	E1	Rhophilin-2 PDZ	G9	LNX1 PDZ3
B6	NHERF-2 PDZ2	E2	Harmonin PDZ1	G10	LNX1 PDZ4
B7	PSD-95 PDZ1+2	E3	Harmonin PDZ2	G11	LNX2 PDZ1
B8	PSD-95 PDZ3	E4	Neurabin PDZ	G12	LNX2 PDZ2
B9	CNRasGEF PDZ	E5	Spinophilin PDZ	H1	LNX2 PDZ4
B10	CAL PDZ	E6	α1-syntrophin PDZ	H2	PTPN4 PDZ
B11	nNOS PDZ	E7	ß1-syntrophin PDZ	H3	Rho-GEF PDZ
B12	INADL PDZ5	E8	ß2-syntrophin PDZ	H4	RA-GEF PDZ
C1	INADL PDZ6	E9	γ1-syntrophin PDZ	H5	Enigma PDZ
C2	SAP97 PDZ1+2	E10	γ2-syntrophin PDZ	H6	LARG PDZ
C3	SAP97 PDZ3	E11	PAPIN PDZ	H7	PTPN3 PDZ
C4	SAP102 PDZ1+2	E12	MAST-205 PDZ	H8	Shank1 PDZ
C5	SAP102 PDZ3	F1	MUPP1 PDZ1	H9	Tamalin PDZ
C6	Chap110 PDZ1+2	F2	MUPP1 PDZ6	H10	PAR-3 PDZ1
C7	Chap110 PDZ3	F3	MUPP1 PDZ7	H11	PAR-3 PDZ2
C8	E6TP1 PDZ	F4	MUPP1 PDZ8	H12	PAR-3 PDZ3

FIGURE 1. **The β_1AR-CT binds selectively to specific PDZ domains.** Equal amounts (1 μg) of purified His-tagged fusion proteins corresponding to 96 distinct PDZ domains were spotted on nylon membranes. An overlay with β_1AR-CT-GST (100 nM) revealed strong and specific binding to several PDZ domains, including PSD-95 PDZ3, CAL PDZ, MAGI-1 PDZ1, MAGI-2 PDZ1, MAGI-2 PDZ2, MAGI-3 PDZ1, SAP97 PDZ3, and GIPC PDZ. The data shown here are representative of eight independent experiments.

when co-expressed with wild-type β_1AR, MAGI-3 was found almost exclusively at the plasma membrane where it co-localized well with β_1AR (Fig. 4, *C–E*). In contrast, no co-localization was observed when MAGI-3 was co-expressed with V477A (Fig. 4, *F–H*), as MAGI-3 remained predominantly targeted to the nucleus and exhibited little if any co-localization with the mutant receptor. Stimulation of the cells with isoproterenol (15 min) had no significant effect of the extent of β_1AR/MAGI-3 co-localization (data not shown). These data confirm the findings from the co-immunoprecipitation experiments that β_1AR and MAGI-3 can interact in cells and, furthermore, reveal that this

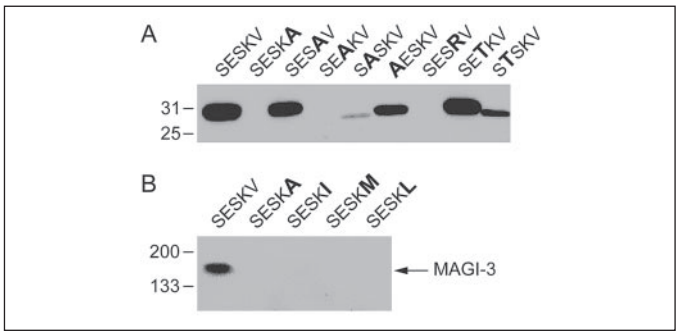

FIGURE 2. **MAGI-3 associates with β_1AR-CT via the ESKV motif of the receptor.** *A*, mutations of the ESKV motif at the β_1AR-CT abolishes binding to MAGI-3 PDZ1. Purified GST fusion proteins (2 μg) corresponding to either the wild-type β_1AR-CT (denoted by its last four amino acids, ESKV) or point-mutated versions of the β_1AR-CT (denoted by sequential replacement of each of the last four amino acids with alanine) were run on SDS-polyacrylamide gels, transferred to nitrocellulose, and overlaid with His/S-tagged MAGI-3 PDZ1 (100 nM). *B*, mutation of the last amino acid of the β_1AR-CT ESKV motif abolishes association with full-length MAGI-3. Purified fusion proteins (2 μg) corresponding to either wild-type β_1AR-CT or mutant versions of β_1AR-CT with substitutions of the last amino acid were adsorbed to glutathione-agarose beads and used to pull down full-length MAGI-3-V5/His from transfected HEK-293 cell lysates. The pulled down MAGI-3 was detected with an anti-V5 antibody via Western blot. The data shown in the two panels of this figure are representative of 3–4 independent experiments. Molecular mass standards (in kDa) are shown on the left.

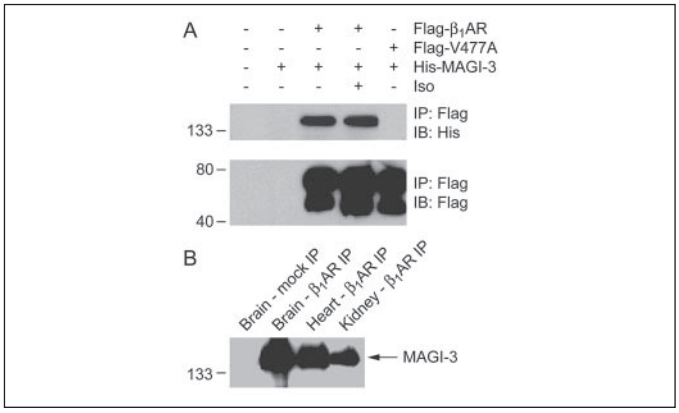

FIGURE 3. **Cellular association of full-length MAGI-3 and full-length β_1AR.** HEK-293 cells were transfected with V5/His-MAGI-3 in conjunction with either Flag-β_1AR wild-type or Flag-β_1AR V477A. Cells were incubated before harvesting in the absence or presence of the β_1AR-selective agonist, isoproterenol (*Iso*, 10 μM, 15 min), as indicated in the figure. Co-immunoprecipitation of MAGI-3 (*top panel*) was apparent under basal conditions (*lane 3*) as well as after the cells had been stimulated with isoproterenol (*lane 4*). Co-immunoprecipitation was not evident, however, when MAGI-3 was co-expressed with the V477A mutant receptor (*lane 5*), revealing the importance of the valine residue at the carboxyl terminus of β_1AR. Empty vector (*lane 1*) and MAGI-3-V5/His alone (*lane 2*) were transfected as negative controls. The *lower panel* reveals the relatively equivalent expression of Flag-β_1AR and Flag-V477A. These data are representative of five independent experiments. *IP*, immunoprecipitation; *IB*, immunoblot. *B*, β_1AR and MAGI-3 interact in native tissues. Solubilized lysates from homogenized rat tissues (heart, brain, and kidney) were subjected to immunoprecipitation with a specific anti-β_1AR antibody. The immunoprecipitated complexes were then probed with an anti-MAGI-3 antibody via Western blot. MAGI-3 was found to robustly co-immunoprecipitate with β_1AR from all three tissues (*lanes 2–4*; $n = 3$ for each tissue). In contrast, MAGI-3 was not detected in samples that were immunoprecipitated using an irrelevant antibody (*first lane*). Molecular mass standards (in kDa) are shown on the left.

interaction results in a striking redistribution of MAGI-3 from the nucleus to the plasma membrane.

MAGI-3 Modulates β_1AR-mediated ERK Activation—We next explored the potential functional significance of the β_1AR/MAGI-3 interaction. Because it has previously been reported that PSD-95 and MAGI-2 strongly regulate β_1AR agonist-promoted internalization, we studied β_1AR endocytosis from the cell surface in the absence and presence of MAGI-3 co-expression. However, β_1AR internalization in response to a 15-min stimulation with isoproterenol (10 μM) was not found to be significantly different when β_1AR was expressed alone

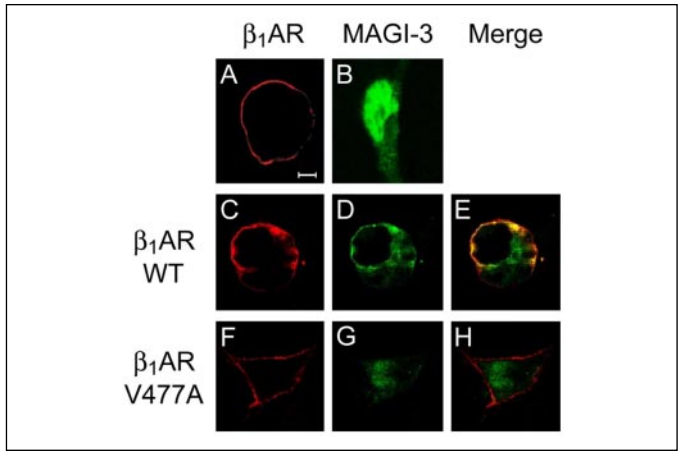

FIGURE 4. **Co-localization of MAGI-3 and wild-type β_1AR but not the V477A mutant receptor in cells.** HEK-293 cells were transiently transfected with FLAG-tagged β_1AR alone (*A*), MAGI-3-V5/His alone (*B*), Flag-β_1AR wild-type plus MAGI-3-V5/His (*C–E*), or Flag-β_1AR mutant (V477A) plus MAGI-3-V5/His (*F–H*). After fixation and permeabilization, cells were stained with a mouse anti-FLAG M2 antibody followed by a Texas Red-conjugated anti-mouse IgG and/or stained with a rabbit anti-His antibody followed by a fluorescein isothiocyanate-conjugated anti-rabbit IgG. Co-localization of wild-type β_1AR with MAGI-3 is revealed in *yellow* following merging of the two individual images, as shown in *E*. These data are representative of 4–6 independent experiments for each condition.

(18 ± 4%) *versus* when β_1AR/MAGI-3 were expressed together (16 ± 5%, $n = 4$). In further functional studies, no differences were observed in cyclic AMP generation following isoproterenol stimulation of β_1AR expressed alone (5.6 ± 1.2-fold over untransfected cells) *versus* β_1AR/MAGI-3 co-expressed (5.1 ± 1.0-fold over untransfected cells, $n = 3$). However, as shown in Fig. 5, co-expression with MAGI-3 had a substantial effect on β_1AR-mediated activation of ERK. Isoproterenol-stimulated ERK activation was more than 6-fold for β_1AR expressed alone but less than 4-fold when β_1AR and MAGI-3 were co-expressed (Fig. 5*A*). In contrast, no significant effect of MAGI-3 co-transfection was observed on the ability of the V477A mutant receptor to couple to ERK activation (Fig. 5*B*). A quantification of these data is presented in Fig. 5*C*. The magnitude of the attenuation of β_1AR-mediated ERK activation by MAGI-3 was comparable at three different time points (Fig. 5*D*). Western blot analyses revealed that MAGI-3 co-expression had no effect on the total expression levels of β_1AR and also revealed that wild-type β_1AR and the V477A mutant receptor were expressed at comparable levels. The stimulation of ERK phosphorylation induced by both wild-type and mutant β_1AR was completely blocked by pretreatment of the cells with pertussis toxin, which indicates a requirement for β_1AR coupling to G_i/G_o in this signaling pathway (data not shown). These data suggest that the ability of MAGI-3 to modulate β_1AR coupling to G_i/G_o and downstream ERK activation is dependent on the physical interaction between β_1AR and MAGI-3.

Differential PDZ Domain Interactions of β_1AR and β_2AR—β_1AR and β_2AR exhibit a high degree of sequence similarity, and even their carboxyl-terminal motifs (ESKV for β_1AR *versus* DSLL for β_2AR) are roughly similar, featuring acidic residues at the −3 positions, Ser residues at the −2 positions, and hydrophobic residues with long aliphatic side chains at the terminal positions. To examine whether there may be any overlap between β_1AR and β_2AR in their interactions with PDZ domains, overlays of the PDZ domain array were performed with fusion proteins corresponding to the carboxyl termini of both receptors. As described above, β_1AR-CT interacted with MAGI-1 PDZ1, MAGI-2 PDZ1/2, MAGI-3 PDZ1, PSD-95 PDZ3, SAP97 PDZ3, CAL PDZ, and GIPC PDZ (shown earlier in Fig. 1). In contrast, overlays of the PDZ array with β_2AR-CT resulted in a pattern of binding completely distinct

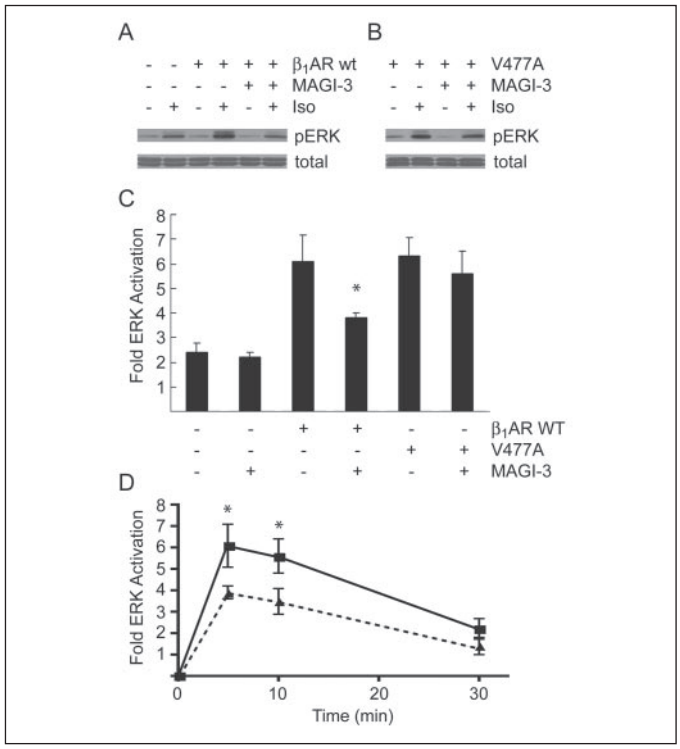

FIGURE 5. **MAGI-3 specifically inhibits β_1AR-stimulated ERK activation.** COS-7 cells were transiently transfected with Flag-β_1AR, Flag-V477A mutant receptor, and/or V5/His-MAGI-3. Twenty-four to forty-eight hours after transfection, cells were treated with serum-free medium overnight. Serum-starved cells were stimulated with 10 μM isoproterenol (*Iso*) for 5 min at 37 °C. ERK activation was assayed as described under "Experimental Procedures." Expression of MAGI-3 was found to dramatically inhibit β_1AR-mediated ERK activation (*A*) but have little effect on ERK activation by the V477A mutant receptor (*B*). *C*, quantification of the effect of MAGI-3 on β_1AR- and V477A-mediated ERK activation. The amount of phospho-ERK immunoreactivity observed following isoproterenol stimulation was expressed as a fold of the phospho-ERK immunoreactivity in the absence of stimulation. *D*, time course of the effect of MAGI-3 on β_1AR-mediated ERK activation. The results from cells transfected with β_1AR alone are indicated by the *squares* and *solid line*, whereas the results from cells co-transfected with β_1AR/MAGI-3 are indicated by the *triangles* and *dashed line*. For both *C* and *D*, the data and error bars represent means ± S.E. for three independent experiments. The *asterisks* indicate a significant decrease ($p < 0.05$) relative to phospho-ERK immunoreactivity in the absence of transfected MAGI-3. *WT*, wild-type.

from that observed for β_1AR-CT. As shown in Fig. 6*A*, β_2AR-CT bound strongly to NHERF-1 PDZ1, NHERF-2 PDZ1, NHERF-2 PDZ2, and PDZK1 PDZ2 but bound only weakly or not at all to other PDZ domains on the array. To study the importance of the terminal amino acid in mediating this difference in PDZ binding specificity between β_1AR-CT and β_2AR-CT, the aforementioned β_1AR-CT point mutant with the terminal Val mutated to Leu (ESKL) was utilized to mimic the terminal position of β_2AR. Strikingly, this mutant did not detectably bind to any of the PDZ domains that bound well to the wild-type β_1AR-CT. Instead, the ESKL mutant bound strongly to NHERF-1 PDZ1, NHERF-2 PDZ2, PDZK2 PDZ2, and also bound weakly to MAGI-3 PDZ5 (Fig. 6*B*), whereas mutation of the terminal Val residue to Ala (ESKA) resulted in a fusion protein that did not bind strongly to any of the PDZ domains on the array (data not shown). These data emphasize the specificity of binding between PDZ domains and their targets, as a single point mutation to the β_1AR-CT resulted in a switch of its PDZ domain binding specificity to a profile much more comparable with that of the β_2AR-CT.

DISCUSSION

Interactions between the β_1-adrenergic receptor and Class I PDZ domain-containing proteins have been uncovered previously via several different techniques. β_1AR interactions with PSD-95 (3) and GIPC (7) were identified in yeast two-hybrid screens, whereas associations with MAGI-2 (4), CNrasGEF (6), and CAL (8) were identified via biochemical approaches. To get as comprehensive a view as possible of β_1AR/PDZ interactions, we turned to a proteomic approach in which most known or putative Class I PDZ domains were expressed as fusion proteins and arranged in a proteomic array. Screens of this array with β_1AR-CT revealed interactions with most of the previously reported PDZ partners of β_1AR, as well as associations with two novel partners, SAP97 and MAGI-3. The interaction with MAGI-3 was shown to occur in cells and to exert significant effects on β_1AR signaling, thereby validating the use of the proteomic PDZ array as a means of identifying physiologically relevant interactions between PDZ scaffolds and transmembrane proteins, such as β_1AR, that possess potential PDZ-interacting motifs. β_1AR is known to regulate cellular physiology primarily by coupling to G_s, but disruption of β_1AR/PDZ interactions in cardiac myocytes has been shown to result in dramatically increased coupling of the receptor to G_i (18). The relevant PDZ interaction underlying this effect has not been conclusively identified, although it has been shown in COS-7 cells that β_1AR association with GIPC leads to decreased G_i-mediated ERK activation by β_1AR (7). Interestingly, our data reported here reveal that MAGI-3 interaction with β_1AR also strongly impairs G_i-mediated ERK activation by β_1AR. These findings reveal that inhibition of G_i coupling to β_1AR is not unique to GIPC, but can also be mediated by other PDZ partners of β_1AR. It is possible that such alterations in receptor coupling to G proteins may occur through allosteric changes in the accessibility of the G protein binding pocket of the receptor following receptor association with PDZ proteins. MAGI-3 is known to be abundantly expressed in cardiac tissue (19); thus β_1AR interaction with MAGI-3 in cardiac myocytes may contribute to the previously observed importance of the β_1AR PDZ-interacting motif in modulating β_1AR coupling to G proteins in this native cell type (18).

In addition to demonstrating regulation of β_1AR by MAGI-3, our studies also revealed a converse regulation of MAGI-3 by β_1AR. Specifically, co-expression with β_1AR resulted in a striking translocation of MAGI-3 to the plasma membrane, whereas MAGI-3 expressed alone exhibited a predominantly nuclear localization. MAGI-3 was first identified only several years ago (19), and little is known at present about the set of cellular proteins with which MAGI-3 can interact. Given the fact that we and others (20) have observed strong MAGI-3 expression in the nuclei of certain cell types, it is tempting to speculate that MAGI-3 may bind to various partners in the nucleus and play a role in transcriptional regulation, as has been shown to be the case for other PDZ scaffolds (21–24). If MAGI-3 does have a physiological role in the nucleus, then the control of MAGI-3 localization via association with transmembrane proteins such as β_1AR may represent a novel and specific mechanism by which such PDZ-interacting transmembrane proteins can influence nuclear function.

Our screens of the PDZ array revealed that β_2AR interacts with a narrow set of PDZ partners entirely distinct from the set of PDZ domains bound by β_1AR. These findings are consistent with the fact that β_2AR has been previously reported to associate with NHERF-1 (9–11) and NHERF-2 (10) but not with any other PDZ partners. Interestingly, mutation of the last amino acid of the β_1AR-CT to match the last amino acid of β_2AR-CT resulted in a striking change in β_1AR/PDZ interactions, with the β_1AR-CT now exhibiting strong binding to the NHERF PDZ domains instead of its normal set of PDZ partners. This observation emphasizes the specificity of interactions between GPCRs and their associated PDZ scaffolds. β_1AR and β_2AR are known to bind the same endogenous ligands and couple to the same G proteins but yet are also known to exert significantly different effects on cellular physi-

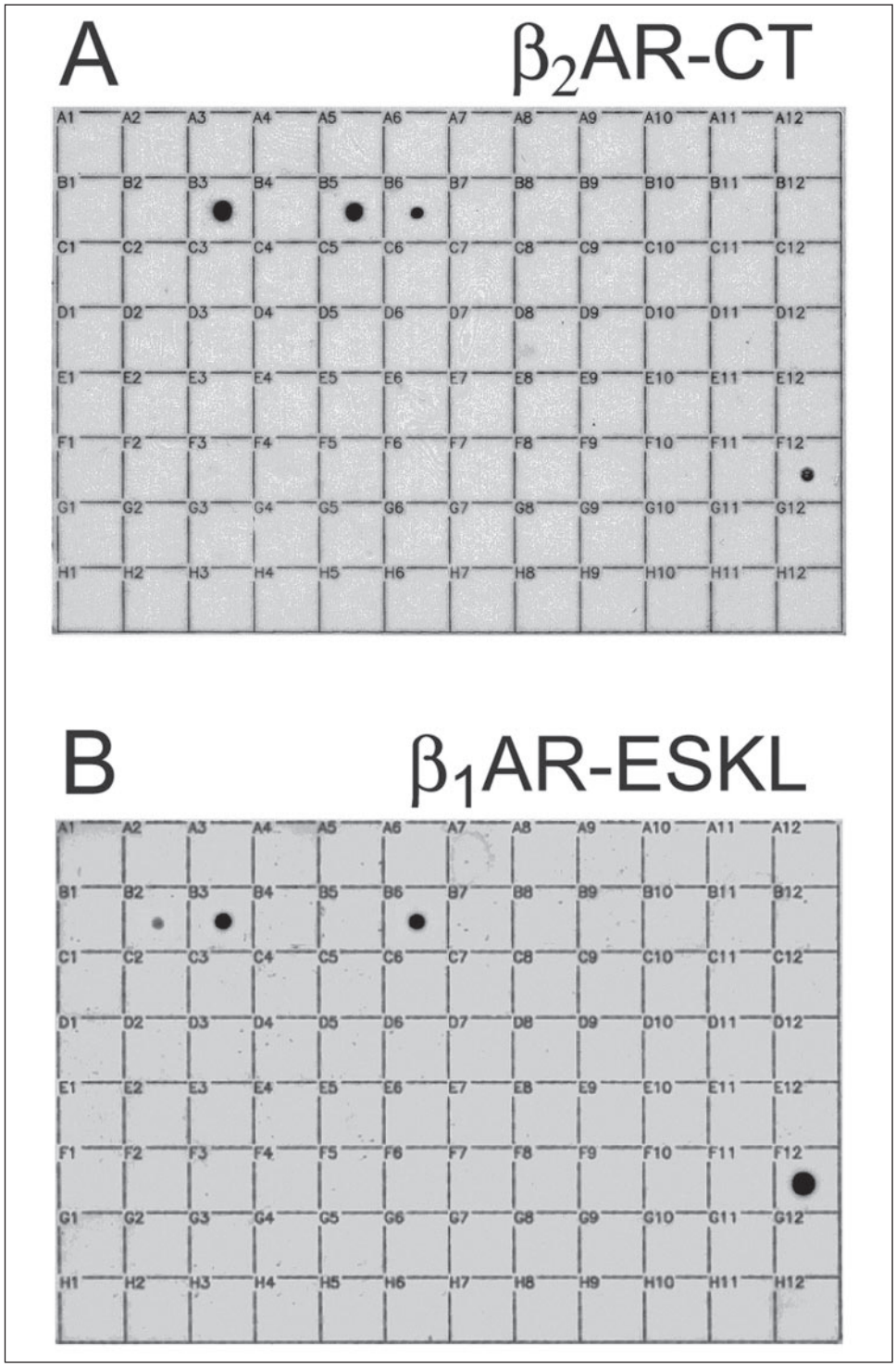

FIGURE 6. **Switch of β_1AR-CT binding specificity to a β_2AR-like profile via mutation of the terminal amino acid.** Equal amounts (1 μg) of purified His-tagged fusion proteins corresponding to 96 distinct PDZ domains were spotted on nylon membranes. Overlay with GST fusion proteins (100 nM) corresponding to either the β_2AR-CT (*A*) or a point-mutated version of the β_1AR-CT (denoted in *B* by replacement of the terminal valine residue with leucine, *ESKL*) resulted in a switch of the β_1AR-CT binding specificity to a profile more similar to that of the β_2AR-CT. These data are representative of 3–5 independent experiments for each condition.

ology in certain cell types (2, 25–32). The association of the two receptors with unique sets of PDZ scaffolds is likely a key factor that underlies the distinct cellular actions of β_1AR and β_2AR.

Differential association with PDZ scaffolds represents both a potential molecular explanation for differences between βAR subtypes and also a probable mechanism underlying cell-specific differences in β_1AR signaling and trafficking. Like most GPCRs, β_1AR exhibits marked variation in its behavior in distinct cell types, with substantial differences in the rate and extent of agonist-promoted internalization being especially notable (12–15). Most PDZ scaffolds are not expressed uniformly across all tissues but instead tend to exhibit profound differences in expression levels between different tissues and cell types (1). Thus, interactions of GPCRs such as β_1AR with PDZ scaffolds that exhibit distinctive patterns of expression across different tissues may account for many examples of cell-type specific regulation of GPCR signaling and trafficking.

Acknowledgments—We thank all of the investigators, listed in the supplementary materials, who contributed PDZ constructs toward the development of the PDZ domain array.

REFERENCES

1. Hung, A. Y., and Sheng, M. (2002) *J. Biol. Chem.* **277,** 5699–5702
2. Hall, R. A. (2004) *Semin. Cell Dev. Biol.* **15,** 281–288
3. Hu, L. A., Tang, Y., Miller, W. E., Cong, M., Lau, A. G., Lefkowitz, R. J., and Hall, R. A. (2000) *J. Biol. Chem.* **275,** 38659–38666
4. Xu, J., Paquet, M., Lau, A. G., Wood, J. D., Ross, C. A., and Hall, R. A. (2001) *J. Biol. Chem.* **276,** 41310–41317
5. Hu, L. A., Chen, W., Premont, R. T., Cong, M., and Lefkowitz, R. J. (2002) *J. Biol. Chem.* **277,** 1607–1613
6. Pak, Y., Pham, N., and Rotin, D. (2002) *Mol. Cell Biol.* **22,** 7942–7952
7. Hu, L. A., Chen, W., Martin, N. P., Whalen, E. J., Premont, R. T., and Lefkowitz, R. J. (2003) *J. Biol. Chem.* **278,** 26295–26301
8. He, J., Bellini, M., Xu, J., Castleberry, A. M., and Hall, R. A. (2004) *J. Biol. Chem.* **279,** 50190–50196
9. Hall, R. A., Premont, R. T., Chow, C. W., Blitzer, J. T., Pitcher, J. A., Claing, A., Stoffel, R. H., Barak, L. S., Shenolikar, S., Weinman, E. J., Grinstein, S., and Lefkowitz, R. J. (1998) *Nature* **392,** 626–630
10. Hall, R. A., Ostedgaard, L. S., Premont, R. T., Blitzer, J. T., Rahman, N., Welsh, M. J., and Lefkowitz, R. J. (1998) *Proc. Natl. Acad. Sci. U. S. A.* **95,** 8496–8501
11. Cao, T. T., Deacon, H. W., Reczek, D., Bretscher, A., and von Zastrow, M. (1999) *Nature* **401,** 286–290
12. Suzuki, T., Nguyen, C. T., Nantel, F., Bonin, H., Valiquette, M., Frielle, T., and Bouvier, M. (1992) *Mol. Pharmacol.* **41,** 542–548
13. Green, S. A., and Liggett, S. B. (1994) *J. Biol. Chem.* **269,** 26215–26219
14. Tang, Y., Hu, L. A., Miller, W. E., Ringstad, N., Hall, R. A., Pitcher, J. A., DeCamilli, P., and Lefkowitz, R. J. (1999) *Proc. Natl. Acad. Sci. U. S. A.* **96,** 12559–12564
15. Shiina, T., Kawasaki, A., Nagao, T., and Kurose, H. (2000) *J. Biol. Chem.* **275,** 29082–29090
16. Fam, S. R., Paquet, M., Castleberry, A. M., Oller, H., Lee, C. J., Traynelis, S. F., Smith, Y., Yun, C. C., and Hall, R. A. (2005) *Proc. Natl. Acad. Sci. U. S. A.* **102,** 8042–8047
17. Balasubramanian, S., Teissere, J. A., Raju, D. V., and Hall, R. A. (2004) *J. Biol. Chem.* **279,** 18840–18850
18. Xiang, Y., Devic, E., and Kobilka, B. (2002) *J. Biol. Chem.* **277,** 33783–33790
19. Wu, Y., Dowbenko, D., Spencer, S., Laura, R., Lee, J., Gu, Q., and Lasky, L. A. (2000) *J. Biol. Chem.* **275,** 21477–21485
20. Adamsky, K., Arnold, K., Sabanay, H., and Peles, E. (2003) *J. Cell Sci.* **116,** 1279–1289
21. Hsueh, Y. P., Wang, T. F., Yang, F. C., and Sheng, M. (2000) *Nature* **404,** 298–302
22. Kanai, F., Marignani, P. A., Sarbassova, D., Yagi, R., Hall, R. A., Donowitz, M., Hisaminato, A., Fujiwara, T., Ito, Y., Cantley, L. C., and Yaffe, M. B. (2000) *EMBO J.* **19,** 6778–6791
23. Balda, M. S., and Matter, K. (2000) *EMBO J.* **19,** 2024–2033
24. Wang, G. S., Hong, C. J., Yen, T. Y., Huang, H. Y., Ou, Y., Huang, T. N., Jung, W. G., Kuo, T. Y., Sheng, M., Wang, T. F., and Hsueh, Y. P. (2004) *Neuron* **42,** 113–128
25. Xiao, R. P., and Lakatta, E. G. (1993) *Circ. Res.* **73,** 286–300
26. Xiao, R. P., Hohl, C., Altschuld, R., Jones, L., Livingston, B., Ziman, B., Tantini, B., and Lakatta, E. G. (1994) *J. Biol. Chem.* **269,** 19151–19156
27. Communal, C., Singh, K., Sawyer, D. B., and Colucci, W. S. (1999) *Circulation* **100,** 2210–2212
28. Zaugg, M., Xu, W., Lucchinetti, E., Shafiq, S. A., Jamali, N. Z., and Siddiqui, M. A. (2000) *Circulation* **102,** 344–350
29. Chesley, A., Lundberg, M. S., Asai, T., Xiao, R. P., Ohtani, S., Lakatta, E. G., and Crow, M. T. (2000) *Circ. Res.* **87,** 1172–1179
30. Devic, E., Xiang, Y., Gould, D., and Kobilka, B. (2001) *Mol. Pharmacol.* **60,** 577–583
31. Shizukuda, Y., and Buttrick, P. M. (2002) *J. Mol. Cell Cardiol.* **34,** 823–831
32. Cesetti, T., Hernandez-Guijo, J. M., Baldelli, P., Carabelli, V., and Carbone, E. (2003) *J. Neurosci.* **23,** 73–83